Cnoidal wave patterns in quadratic nonlinear media

Yaroslav V. Kartashov,[1,2] Victor A. Vysloukh,[3] and Lluis Torner[1]
[1]*ICFO–Institute de Ciencies Fotoniques, and Department of Signal Theory and Communications, Universitat Politecnica de Catalunya, 08034 Barcelona, Spain*
[2]*Physics Department, M. V. Lomonosov Moscow State University, 119899 Moscow, Russia*
[3]*Departamento de Fisica y Matematicas, Universidad de las Americas–Puebla, Santa Catarina Martir, 72820 Puebla, Cholula, Mexico*
(Received 17 December 2002; revised manuscript received 4 April 2003; published 27 June 2003)

We report the existence of whole families of stationary cnoidal, periodic wave patterns in quadratic nonlinear media. We study the main physical features of the multicolored light patterns, including their shape, contrast, multifrequency energy sharing, asymptotics in the cascading limit, and excitation. Our numerical simulations predict that the cnoidal waves with high and even with moderate contrasts are robust enough against modulational instabilities to be experimentally observable.

DOI: 10.1103/PhysRevE.67.066612 PACS number(s): 42.65.Tg, 42.65.Wi, 42.65.Jx

During the past years, spatial and temporal solitons supported by quadratic nonlinearities, first predicted in the 1970s [1], have been theoretically investigated and observed experimentally in several materials and parametric wave interactions (for summaries of experimental observations and salient theoretical results, see, e.g., Refs. [2–4]), and thus their basic properties are now well established. Bright solitons are fully localized solutions of the equations governing the light evolution in the quadratic crystal, and while more complex solitary-wave structures (bright-dark, multiple-peaked, twin-hole, embedded, etc.) solutions of such equations have been found (see, for example, Refs. [4,5]), only single bright solitons, which feature a single energy peak and realize the minimum of the system Hamiltonian, have been found to be dynamically stable. Thus, a crucial open question is whether more complex, multipeaked self-sustained light patterns can be built that are robust enough to be experimentally observable.

Here we study the process of second-harmonic generation (SHG) and report the existence of whole families of self-sustained periodical patterns, or *multicolor cnoidal wave patterns*, which correspond to doubly periodic mutually trapped fundamental frequency and second-harmonic beams or pulses. Cnoidal waves have been studied in detail in cubic nonlinear media [6–8], including Bose-Einstein condensates with a periodic potential [9], during the past few years. In quadratic nonlinear media, only zero-parameter analytical periodic solutions have been obtained, e.g., with the aid of the Hamiltonian formalism [10], direct substitution [11], and Lie group analysis [12]. General families of cnoidal waves are reported here, for the first time to our knowledge. The families of cnoidal waves come with different local and global shapes, and with varying localization degrees, and we find that multicolored cnoidal patterns existing with a moderate or high localization appear to be robust enough to allow their experimental generation and exploration. Here we report our findings for the cnoidal waves of simplest types, defined by their so-called cn-, dn-, and sn-type asymptotics in the cascading (large phase-mismatch) limit, in the case of one-dimensional light propagation in noncritical two-wave second-harmonic generation, but the results are relevant and can be extended to more general settings.

The propagation of slowly varying envelopes of the fundamental frequency and second-harmonic light beams or pulses in weakly anisotropic quadratic nonlinear media under conditions for noncritical type-I phase-matching SHG is described by the system of reduced equations [4,5]

$$i\frac{\partial q_1}{\partial \xi}=\frac{d_1}{2}\frac{\partial^2 q_1}{\partial \eta^2}-q_1^* q_2\exp(-i\beta\xi),$$
$$i\frac{\partial q_2}{\partial \xi}=\frac{d_2}{2}\frac{\partial^2 q_2}{\partial \eta^2}-q_1^2\exp(i\beta\xi). \tag{1}$$

Here

$$q_1=(2k_1/k_2)^{1/2}(2\pi\omega_0^2\chi^{(2)}r_0^2/c^2)A_1,$$
$$q_2=(2\pi\omega_0^2\chi^{(2)}r_0^2/c^2)A_2$$

are normalized complex amplitudes of the fundamental ($\omega=\omega_0$) and second-harmonic ($\omega=2\omega_0$) waves; $k_1=k(\omega_0)$; $k_2=k(2\omega_0)\approx 2k_1$; $A_{1,2}(\eta,\xi)$ are the slowly varying amplitudes; r_0 is the transverse scale of the input beams or pulses; $\eta=x/r_0$ is the normalized transverse coordinate; $\xi=z/(k_1 r_0^2)$ is the normalized propagation distance; $\beta=(2k_1-k_2)k_1 r_0^2$ is the phase-mismatch parameter; $d_1=-1$; $d_2=-k_1/k_2\approx-\frac{1}{2}$. We are looking for stationary periodic phase-locked solution of Eq. (1) in the form $q_{1,2}(\xi,\eta)=w_{1,2}(\eta)\exp(ib_{1,2}\xi)$, where $w_{1,2}(\eta)$ are real functions, and $b_{1,2}$ are real constants which physically correspond to the phase shifts induced by the nonlinear wave interaction. Under the assumption $b_2=\beta+2b_1$, necessary for the solutions to be stationary and to avoid any power exchange between the waves, the resulting system of equations takes the form

$$\frac{d^2 w_1}{d\eta^2}-2b_1 w_1+2w_1 w_2=0,$$
$$\frac{d^2 w_2}{d\eta^2}-4(\beta+2b_1)w_2+4w_1^2=0, \tag{2}$$

which, in contrast to the case of fully localized soliton solutions, will be solved together with periodic boundary conditions.

It is well known that Eqs. (2) take a simpler form in the so-called cascading limit, when $|\beta| \gg 1$ and the field amplitudes are such that there is a negligible conversion between the fundamental wave and second harmonic. Making use of the substitution $w_2(\eta) = w_1^2(\eta)/(\beta + 2b_1)$ for the second-harmonic field in this limit, one arrives at the nonlinear Schrödinger equation

$$\frac{d^2 w_1}{d\eta^2} - 2b_1 w_1 + \frac{2w_1^3}{(\beta + 2b_1)} = 0. \tag{3}$$

This equation describes cnoidal waves in Kerr media, and is thus known to admit two periodic cnoidal wave solutions at positive phase mismatch $\beta \gg 1$ (so-called *dn wave* and *cn wave*) [6]:

$$w_1(\eta) = (\beta + 2b_1)^{1/2} \mathrm{dn}(\eta, m),$$

$$m = (2 - 2b_1)^{1/2}, \quad \tfrac{1}{2} \leqslant b_1 \leqslant 1,$$

$$w_1(\eta) = m(\beta + 2b_1)^{1/2} \mathrm{cn}(\eta, m),$$

$$m = (b_1 + 1/2)^{1/2}, \quad -\tfrac{1}{2} \leqslant b_1 \leqslant \tfrac{1}{2}, \tag{4}$$

and one solution at negative phase mismatch $\beta \ll -1$ (so-called *sn wave*),

$$w_1(\eta) = m|\beta + 2b_1|^{1/2} \mathrm{sn}(\eta, m),$$

$$m = (-2b_1 - 1)^{1/2}, \quad -1 \leqslant b_1 \leqslant -\tfrac{1}{2}. \tag{5}$$

Here $\mathrm{dn}(\eta, m)$, $\mathrm{cn}(\eta, m)$, and $\mathrm{sn}(\eta, m)$ are the elliptic Jacobi functions, where m is the modulus of the elliptic function. The period T of the cn and sn waves amounts to $4K(m)$, while the period of the dn wave is $2K(m)$. In both cases, $K(m)$ is the elliptic integral of the first kind. When the parameter $m \to 0$ (which physically corresponds to weak localization), the cn and sn waves transform into small amplitude harmonic waves, where as when $m \to 1$ (limit of strong localization) these waves transform into an array of out-of-phase bright and dark solitons, respectively. The dn wave at $m \to 0$ transforms into a plane wave, and at $m \to 1$ into an array of in-phase solitons.

Multicolored cnoidal waves with genuine quadratic features occur for small phase mismatch and at exact phase matching. To obtain the stationary cnoidal wave profiles in such cases, we solved Eqs. (2) numerically by using a relaxation method with periodic boundary conditions. In most cases, expressions (4) and (5) served as good initial guess for the relaxation method, since the difference between the exact solution and the approximate one is small for $|\beta| \geqslant 10$. As $|\beta| \to 0$, amplitudes of the fundamental wave and second harmonic become comparable. Numerical integration shows that at $|\beta| \sim 1$, profile of the sn wave becomes rather complicated due to the appearance of high-frequency oscillations on the otherwise smooth profile, and the corresponding families of solutions intermix with complex higher-order solutions. Therefore, in this paper we concentrate solely on the dn and cn waves, which are the families more relevant from an experimental point of view. A comprehensive study of the sn-wave families, as well as of the rich sets of existing higher-order solutions will be published elsewhere in the future. Mathematically, for a fixed mismatch β, the cnoidal waves are defined by two free parameters, namely, the transverse period T, and the nonlinear shift b_1 (propagation constant). Physically, the latter is linked to the energy flowing inside each transverse wave period. Since one can use scaling transformations to obtain cnoidal waves with different periods from a given solution family, from now on we fix the wave period to $T = 2\pi$ and vary the nonlinear shift b_1 (for different material mismatches).

The main properties of the families of the dn waves are summarized in Fig. 1. Both components $w_{1,2}$ of this wave never vanish. Thus, there spectra always contain a dc component. The dependence of the energy flow per period,

$$U = \int_0^T [w_1^2(\eta) + w_2^2(\eta)] d\eta, \tag{6}$$

on the propagation constant b_1 for the dn wave is shown in Fig. 1(a). At positive β, the energy flow monotonically increases with increasing propagation constant. At low enough negative β, the energy flow becomes a nonmonotonic function of b_1. There exists a cutoff on propagation constant for the dn wave that is clearly seen in Fig. 1(a). At the cutoff, the dn wave transforms into a plane wave. The dependence of the cutoff propagation constant on the phase mismatch is shown in Fig. 1(b). One can see that at negative β, the cutoff value of the propagation constant is proportional to $|\beta|$. When the energy flow increases, the dn wave transforms into an array of in-phase localized solitons.

A characteristic feature of cnoidal waves is their *degree of localization*, or contrast, defined as

$$V_{1,2} = \frac{|w_{1,2}|_{\max} - |w_{1,2}|_{\min}}{|w_{1,2}|_{\max} + |w_{1,2}|_{\min}}. \tag{7}$$

This parameter shows how the cnoidal waves link the fully delocalized solutions (small periodic modulations of plane waves) and the fully localized light patterns (arrays of high energy single solitons). The former limit corresponds to $V_{1,2} = 0$, the second to $V_{1,2} = 1$. The dependence of this parameter on the energy flow and mismatch for the dn wave is shown in Figs. 1(c) and 1(d). In the case of the dn-waves, increase of $V_{1,2}$ from 0 to 1 corresponds to the transformation of the dn wave from plane wave (that is modulationally unstable in quadratic media) into an array of well-localized in-phase fundamental solitons (which are known to be stable). Thus, on physical grounds, the value of $V_{1,2}$ is directly related to the potential stability or instability of the corresponding light patterns. Intuitively, the closer $V_{1,2}$ is to unity, the more dynamically stable the corresponding cnoidal wave is expected to be. Notice that at positive β, the contrast of the second-harmonic wave is always higher than that of the fundamental wave, and that $V_{1,2}$ are monotonically increasing functions of the energy flow. At $\beta = -3$, at weak

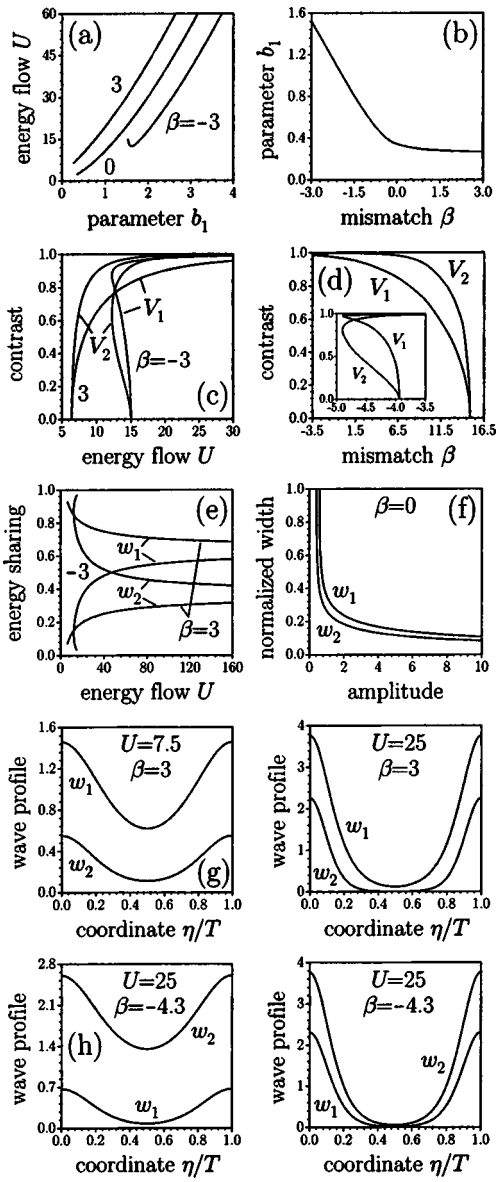

FIG. 1. Properties of the dn wave with period $T=2\pi$. (a) Energy flow U as a function of propagation constant b_1 for various phase mismatches β. (b) Propagation constant cutoff versus phase mismatch. (c) Wave contrast as a function of energy flow U for two values of phase mismatch, and (d), wave contrast as a function of phase mismatch at $U=25$. (e) Energy sharing between the fundamental wave and second harmonic versus total energy flow for two values of phase mismatch. (f) Amplitude-width diagram at $\beta=0$. Rows (g) and (h) show typical profiles of the dn wave.

localization the contrast can become a two-valued function of energy flow [this is connected to the nonmonotonic dependence $U(b_1)$] and at high localization V_1 can amount to higher values than V_2. Dependence of the contrast on phase mismatch at fixed energy flow U [Fig. 1(d)] shows that there are cutoff conditions at both positive and negative β.

Another important parameter is the energy sharing per transverse period between the fundamental and second-harmonic waves, defined as

$$S_{1,2}=\frac{\int_0^T w_{1,2}^2(\eta)d\eta}{\int_0^T[w_1^2(\eta)+w_2^2(\eta)]d\eta}. \tag{8}$$

One can see from Fig. 1(e) that depending on the sign of the phase mismatch at low energy levels, most part of the wave energy can be concentrated either in the fundamental wave ($\beta>0$) or in the second harmonic ($\beta<0$). At high energy flows, most part of the energy is concentrated in the fundamental wave in both cases. Figure 1(f) shows the amplitude-width diagrams for the dn wave at $\beta=0$. The width is defined as the full width at half maximum of the field intensity $(w_{1,2}^2)_{\max}$, and has been plotted normalized to the wave period T. Notice that because the dn wave is transformed into a plane wave as $b_1\to 0$, the width can be properly calculated only above a certain minimal amplitude; however, only amplitudes well above such values are of physical interest. At exact phase matching, the width is a monotonically decreasing function of amplitude. Finally, rows (g) and (h) from Fig. 1 illustrate the profiles of the dn waves for various values of the energy flows and phase mismatches. The transformation of the wave into an array of the in-phase solitons at high energy flows is clearly visible in the plots.

The salient properties of the cn wave are summarized in Fig. 2. For this wave, w_1 periodically changes its sign, whereas w_2 never vanishes, and, hence, always contains a constant background. The dependence of the energy flow on propagation constant is shown in Fig. 2(a). There exists a cutoff on propagation constant at low energy levels. For $-\infty<\beta\leqslant 1$, the cutoff is given by $b_1=-\beta/2$. At this point the fundamental wave vanishes, $w_1\to 0$, whereas the second harmonic transforms into a wave of constant amplitude, $w_2\to(1-\beta)/2$. For $\beta>1$, the cutoff always equals $b_1=-\frac{1}{2}$ and both the fundamental wave and second harmonic vanish at this point. For positive phase mismatches, the energy flow is a monotonically increasing function of propagation constant, however, at small enough negative β this dependence can have a minimum. With increase of energy flow, the constant background in second harmonic decreases and the cn wave transforms into an array of out-of-phase localized bright solitons. This process is clearly seen from the dependence of wave contrast on energy flow [Fig. 2(b)]. Notice that since the fundamental wave periodically changes its sign, one has $V_1\equiv 1$ always, thus we plotted only V_2 for the second harmonic. An important point is that for the cn waves, the contrast increases slower than that for the dn wave when increasing U. The energy sharing between the fundamental and second-harmonic waves versus energy flow is shown in Fig. 2(d). As in the case of the dn wave at low energy levels, most part of the energy is carried either by the fundamental wave (at positive mismatch) or by the second harmonic (at negative mismatch). Amplitude-width diagram for the cn wave at $\beta=0$ is shown in Fig. 2(e). In the low amplitude limit, the width of the fundamental wave equals $T/4$, whereas the width of the second harmonic is given by $T/2$. Typical profiles of the cn waves are shown in rows (f) and (g) of Fig. 2. The transformation of the waves into arrays of out-of-phase solitons at high localization is clearly apparent.

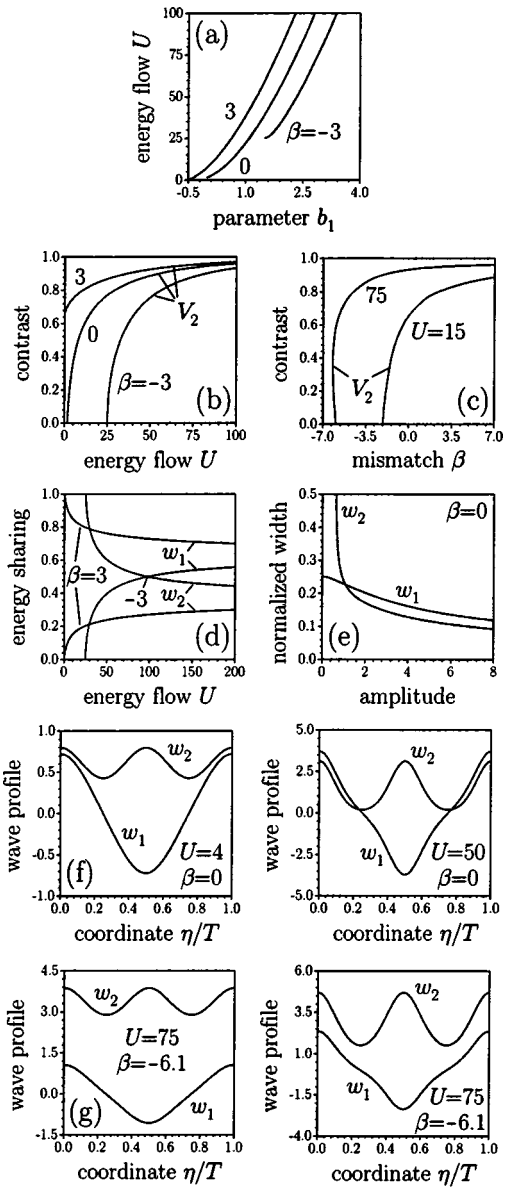

FIG. 2. Properties of the cn wave with period $T=2\pi$. (a) Energy flow U as a function of propagation constant b_1 for various phase mismatches β. (b) Wave contrast as a function of energy flow U for various phase mismatches, and (c), wave contrast as a function of phase mismatch at different energy flows. (d) Energy sharing between the fundamental wave and second harmonic versus total energy flow for two values of phase mismatch. (e) Amplitude-width diagram at $\beta=0$. Rows (f) and (g) show typical profiles of the cn wave.

From the point of view of experimental observation and potential practical applications, the crucial problem is the stability and robustness of the cnoidal wave patterns. In the case of cubic nonlinearity, it is known that $(1+1)$-dimensional dn and cn waves are unstable and only the sn wave is stable, whereas in $(2+1)$ dimensions all types of cnoidal waves are subjected to transverse modulational instability [6–8]. However, it is also known that the perturbation growth rate decays exponentially when the localization of the waves increases, a property that made possible the

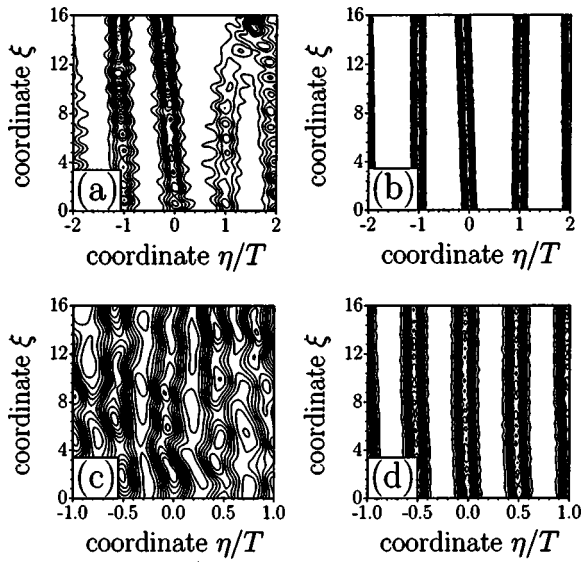

FIG. 3. Propagation of cnoidal waves in a quadratic medium in the presence of Gaussian noise with variance $\sigma_{1,2}^2=0.01$. dn wave with $U=7.5$ (a) and $U=25$ (b) at $\beta=3$. cn waves with $U=2$ (c) and $U=50$ (d) at $\beta=0$. Only the evolution of second-harmonic wave is shown.

experimental observation of cnoidal waves in cubic media [7]. A similar trend is expected for cnoidal waves in quadratic media.

First, we present the outcome of selected series of numerical simulations that show that cnoidal waves with a moderate degree of localization appear to be robust enough to be experimentally observable. Since for both dn and cn waves, the second harmonic contains a constant background, they are expected to be unstable against modulational instabilities. However, as the energy flow increases, the contrast grows. Thus, the constant background decreases, hence the instability growth rate is expected to decrease. Also, an important question regarding the experimental observation of the light patterns is whether they can be excited while embedded in beams with a finite transverse size. To elucidate whether such is the case, we performed numerical simulations by solving Eqs. (1) with input conditions $q_{1,2}(\eta,\xi=0)=[w_{1,2}(\eta)+\rho_{1,2}(\eta)]F(\eta)$, where $w_{1,2}(\eta)$ describe profiles of the stationary waves, $\rho_{1,2}(\eta)$ is a random variable with a Gaussian distribution and variance $\sigma_{1,2}^2$, and the function $F(\eta)$ is a broad Gaussian envelope imposed on the otherwise transversely infinite wave pattern. The width of the envelope was chosen to be much higher than the cnoidal wave period, and we monitored the dynamics of the wave pattern in the center of the envelope. The propagation of the dn wave with a low contrast $V_1=0.41$ (corresponding to the energy flow $U=7.5$) is shown in Fig. 3(a). One can see that the wave pattern is severely affected by the perturbation and self-destroys after a few propagation units, as expected. However, when the energy flow is increased to $U=25$ so that the localization degree amounts to $V_1=0.94$, the wave propagates in a stable way for many propagation units, much larger than those of existing quadratic crystals [Fig. 3(b)]. A similar conclusion was obtained for the cn waves. Figures

3(c) and 3(d) show typical examples. Finally, we notice that because cn waves correspond to the arrays of out-of-phase peaks, they tend to be more robust than the dn waves, where neighboring peaks tend to fuse in the presence of the random perturbations.

Results of numerical simulations with Gaussian noise are fully supported by direct linear stability analysis of periodic cnoidal wave patterns in quadratic medium. Full investigation of stability of cnoidal waves are too complex to be presented here and will be reported in the separate paper. Here we concentrate on one particular case of the dn wave at $\beta=0$. According to the usual procedure, we look for the solution of the system of equations (1) in the form

$$q_{1,2}(\eta,\xi)=[w_{1,2}(\eta)+U_{1,2}(\eta,\xi)+iV_{1,2}(\eta,\xi)]\exp(ib_{1,2}\xi), \tag{9}$$

with $w_{1,2}(\eta)$ being the stationary solutions of Eq. (1), and $U_{1,2}$ and $V_{1,2}$ are, respectively, real and imaginary parts of the small perturbation. Assuming that $U_{1,2}(\eta,\xi)=u_{1,2}(\eta)\exp(\delta\xi)$ and $V_{1,2}(\eta,\xi)=v_{1,2}(\eta)\exp(\delta\xi)$, upon substitution of expression (9) into Eqs. (1) and linearization we arrive at the following equation:

$$\frac{d\Phi}{d\eta}=\mathcal{B}\Phi, \quad \mathcal{B}=\begin{pmatrix}\mathcal{O} & \mathcal{E}\\ \mathcal{N} & \mathcal{O}\end{pmatrix},$$

$$\mathcal{N}=\begin{pmatrix}-2(b_1-w_2)/d_1 & 2w_1/d_1 & -2\delta/d_1 & 0\\ 4w_1/d_2 & -2b_2/d_2 & 0 & -2\delta/d_2\\ 2\delta/d_1 & 0 & -2(b_1+w_2)/d_1 & 2w_1/d_1\\ 0 & 2\delta/d_2 & 4w_1/d_2 & -2b_2/d_2\end{pmatrix}, \tag{10}$$

for perturbation vector $\Phi(\eta)=\{u_1,u_2,v_1,v_2,du_1/d\eta,du_2/d\eta,dv_1/d\eta,dv_2/d\eta\}^T$, where $\mathcal{O}$ and $\mathcal{E}$ are zero and unity 4×4 matrices, respectively. General solution of Eqs. (10) can be expressed in the form $\Phi(\eta)=\mathcal{J}(\eta,\eta')\Phi(\eta')$, where $\mathcal{J}(\eta,\eta')$ is the 8×8 Cauchy matrix. In turn, Cauchy matrix defines the matrix of translation of perturbation eigenvector Φ on one wave period $\mathcal{P}(\eta)=\mathcal{J}(\eta+T,\eta)$. It was rigorously proved in Ref. [7] for the case of cnoidal waves in cubic medium that perturbation eigenvector would be finite along transverse η axis only in the case when the corresponding eigenvalue of the matrix of translation satisfies condition $|\lambda_k|=1$ $(k=1,...,8)$, which gives a receipt of construction of areas of existence of finite perturbations. In contradistinction with the case of localized solitons (where spectrum of perturbations is discrete) for cnoidal waves, one has a band of possible increments at each energy flow. The areas of existence of finite perturbations with real increments are shown in Fig. 4 for the particular case of the dn wave at $\beta=0$. In this case, only two of the eight eigenvalues $\lambda_{1,2}$ of translation matrix have to be taken into account. One can see that such areas shrink with the increase of propagation constant b_1 (energy flow or contrast), so maximal possible increment decreases. Besides perturbations with real increments, perturbations with complex increments are possible (which is the case for the cn waves), however real parts of such increments are usually very small and also found to decrease rapidly with the increase of energy flow. This is in full agreement with the results of numerical simulations of propagation of cnoidal waves in the presence of Gaussian noise.

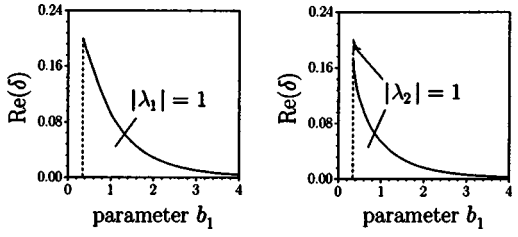

FIG. 4. Areas of existence of finite perturbations with real growth rates for the dn wave at $\beta=0$. Dashed lines in figures correspond to the point where the dn wave transforms into a plane wave.

With regard to the experimental formation of cnoidal waves, we would like to mention that one can use for their excitation arrays of Gaussian beams, or interference patterns produced by intersecting planar wave. Moreover, under appropriate conditions these waves can be formed upon the development of modulational instability of plane waves in quadratic media [13].

In conclusion, we have reported the existence and main properties of several types of lowest-order families of cnoidal waves patterns existing in quadratic nonlinear media. Whole families have been shown to exist for all values of the mismatch. The numerical simulations suggest that multicolored cnoidal wave patterns reported here appear to be robust enough to be experimentally observable (that feature a moderate or a high localization degree). Such patterns of periodic, pixel-like structures might find applications in the fundamental study of complex multicolor light patterns generated by modulational instabilities, and in the practical implementation of optical switching and digital image processing schemes with periodic light patterns, as those demonstrated experimentally recently in quadratic [14,15] and photorefractive [16] materials.

Financial support from CONACyT under Grant No. 34684-E is gratefully acknowledged by Victor A. Vysloukh. Y.V.K. and L.T. acknowledge support by the Generalitat de Catalunya and by the Spanish Government under Contract No. BFM2002-2861.

[1] Yu. N. Karamzin and A. P. Sukhorukov, Sov. Phys. JETP **41**, 414 (1976).
[2] G. I. Stegeman *et al.*, Opt. Quantum Electron. **28**, 1691 (1996).
[3] L. Torner and G. I. Stegeman, Opt. Photonics News **12**, 36 (2001).
[4] A. V. Buryak *et al.*, Phys. Rep. **370**, 63 (2002).
[5] C. R. Menyuk *et al.*, J. Opt. Soc. Am. B **11**, 2434 (1994); A. D. Boardman *et al.*, Phys. Rev. A **52**, 4099 (1995); A. V. Buryak and Yu. S. Kivshar, *ibid.* **51**, R41 (1995); D. Mihalache *et al.*, Opt. Eng. **35**, 1616 (1996); H. He *et al.*, Phys. Rev. E **54**, 896 (1996); M. Haelterman *et al.*, Opt. Lett. **22**, 84 (1997); C. Etrich *et al.*, Opt. Quantum Electron. **30**, 881 (1998); A. R. Champneys *et al.*, Physica D **152–153**, 340 (2001); A. C. Yew *et al.*, J. Nonlinear Sci. **9**, 33 (1999).
[6] V. M. Petnikova *et al.*, Phys. Rev. E **60**, 1 (1999); V. Aleshkevich *et al.*, Opt. Commun. **185**, 305 (2000); J. Opt. Soc. Am. B **18**, 1127 (2001); Quantum Electron. **31**, 257 (2001); F. T. Hioe, Phys. Rev. Lett. **82**, 1152 (1999).
[7] Ya. V. Kartashov *et al.*, Phys. Rev. E **67**, 036613 (2003).
[8] N. Korneev *et al.*, Opt. Commun. **197**, 209 (2001).
[9] L. D. Carr *et al.*, Phys. Rev. A **62**, 063610 (2000); Phys. Rev. E **63**, 066604 (2001); J. C. Bronski *et al.*, Phys. Rev. Lett. **86**, 1402 (2001).
[10] P. Ferro and S. Trillo, Phys. Rev. E **51**, 4994 (1995).
[11] D. F. Parker, J. Opt. Soc. Am. B **15**, 1061 (1998).
[12] S. Lafortune *et al.*, Phys. Rev. E **58**, 2518 (1998).
[13] S. Trillo and P. Ferro, Opt. Lett. **20**, 438 (1995); S. Trillo and S. Wabnitz, Phys. Rev. E **55**, R4897 (1997); R. A. Fuerst *et al.*, Phys. Rev. Lett. **78**, 2756 (1997); H. Fang *et al.*, Opt. Lett. **25**, 1786 (2000); X. Liu *et al.*, Phys. Rev. Lett. **85**, 1871 (2000).
[14] P. Di Trapani and W. Chinaglia, Opt. Lett. **23**, 1653 (1998); A. Bramati *et al.*, *ibid.* **26**, 1409 (2001).
[15] S. Minardi *et al.*, Opt. Lett. **25**, 326 (2000); **27**, 2097 (2002).
[16] Z. Chen and K. McCarthy, Opt. Lett. **27**, 2019 (2002).